ORIGINAL PAPER

In vitro inhibitory profile of NDGA against AChE and its in silico structural modifications based on ADME profile

Chandran Remya · Kalarickal Vijayan Dileep ·
Ignatius Tintu · Elessery Jayadevi Variyar ·
Chittalakkottu Sadasivan

Abstract Acetylcholinesterase (AChE) inhibitors are currently in focus for the pharmacotherapy of Alzheimer's disease (AD). These inhibitors increase the level of acetylcholine in the brain and facilitate cholinergic neurotransmission. AChE inhibitors such as rivastigmine, galantamine, physostigmine and huperzine are obtained from plants, indicating that plants can serve as a potential source for novel AChE inhibitors. We have performed a virtual screening of diverse natural products with distinct chemical structure against AChE. NDGA was one among the top scored compounds and was selected for enzyme kinetic studies. The IC_{50} of NDGA on AChE was 46.2 μM. However, NDGA showed very poor central nervous system (CNS) activity and blood–brain barrier (BBB) penetration. In silico structural modification on NDGA was carried out in order to obtain derivatives with better CNS activity as well as BBB penetration. The studies revealed that some of the designed compounds can be used as lead molecules for the development of drugs against AD

Keywords Acetylcholinesterase · NDGA · ADME · CNS activity · Induced fit docking

Introduction

Alzheimer's disease (AD) is an age related neurodegenerative disease characterized by progressive memory loss and other cognitive impairments. The neuropathology of AD is characterized by extracellular deposition of plaques containing amyloid beta (Aβ) peptides and the presence of intracellular neurofibrillary tangles of tau proteins. The progressive loss of cholinergic neurons leads to reduction in the levels of acetylcholine (ACh), choline acetyltransferase and muscarinic and nicotinic acetylcholine receptors [1, 2]. In addition to this, it has been reported that many cytotoxic signals, such as oxidative stress, inflammation and accumulation of metals at the sites of neurodegeneration, can initiate apoptotic processes [3]. Acetylcholinesterase (AChE) is responsible for the degradation of the neurotransmitter acetylcholine (ACh) in the synaptic cleft of neuromuscular junctions and neuronal contacts in the central nervous system (CNS) [4]. The inhibition of AChE can increase the concentration of ACh, thereby enhancing the cholinergic functions through the activation of synaptic nicotinic receptors [5, 6]. Biochemical studies indicated that AChE can promote amyloid fibril formation by interacting with Aβ peptides through its peripheral anionic site (PAS). It is also reported that the AChE-Aβ complex is more toxic than Aβ peptides alone and the compounds that bind to PAS can slow down the rate of Aβ elicited neurodegeneration [7, 8]. Thus, the inhibition of AChE activity is one of the effective approaches to the symptomatic treatment of AD [9]. AChE inhibitors such as tacrine [10], donepezil [11], galanthamine [12] and rivastigmine [13] have been proved to protect neurons from death in various cell culture models of neurodegenerative diseases and are approved as anti-Alzheimer's drugs [14]. Tacrine and donepezil are from synthetic sources, while galanthamine, rivastigmine, huperzine and physostigmine are from natural sources [15, 16].

A number of experimental results have revealed a connection between neurodegenerative diseases and oxidative stress and also that the free radical accumulation is

C. Remya · K. V. Dileep · I. Tintu · E. J. Variyar ·
C. Sadasivan (✉)
Department of Biotechnology and Microbiology and Inter
University Centre for Biosciences, Kannur University,
Thalassery Campus, Palayad P.O.,
Kerala 670661, India
e-mail: csadasivan@gmail.com

responsible for neuronal injury in a variety of acute and chronic neurological disorders, such as cerebral ischemia and AD [19]. Nordihydroguaiaretic acid (NDGA or 4-[4-(3,4-dihydroxyphenyl)-2,3-dimethylbutyl]benzene-1,2-diol) is a phenolic lignan and a well known antioxidant isolated from the creosote bush, *Larrea tridentates* [17, 18]. It has been reported that NDGA plays a protective role against oxidative stress in cerebellar neurons [20]. It also has a protective role against glutamate and Aβ induced toxicity in cell cultures [21–24]. Hence, NDGA is assumed to be useful against neurological disorders like AD.

Since AD involves multifaceted etiology, its treatment requires multiple drug therapy to address various pathological aspects of the disease. A single compound that exhibits more pharmacological properties such as enhanced cholinergic transmission, inhibition of Aβ accumulation, anti oxidant activity and neuroprotective effects might be more beneficial in the treatment of AD than a compound that exhibits only AChE inhibition. These facts lead to the conclusion that NDGA could be a potential lead compound for the development of drug against AD.

Based on this hypothesis, the AChE inhibitory properties of NDGA were studied in enzyme inhibition assays. An in silico ADME profile of NDGA showed poor blood brain barrier (BBB) penetration and CNS activity. The structure of NDGA was hence modified with an aim to improve BBB penetration and CNS activity. The binding affinity of these modified compounds towards AChE was also determined using molecular modeling and docking methods.

Materials and methods

Screening of natural compounds against AChE

In silico studies were performed using the program suite Schrödinger (http://www.schrodinger.com/). A set of phytochemicals, including alkaloids, phenolics, sterols and terpenes were noted from a published source describing some bioactive compounds and their potential use in the treatment of various diseases such as inflammation, cancer, diabetes mellitus, AIDS and microbial infection [25]. From these, 216 compounds whose interaction with AChE is not yet reported were selected for further studies. The structures of these compounds were collected from the PubChem database (http://pubchem.ncbi.nlm.nih.gov/) and the geometries were optimized using LigPrep module with OPLS-2005 as force field.

The atomic coordinates of human acetylcholinesterase (hAChE) was downloaded from Protein Data Bank (PDB ID: 1B41; http://www.pdb.org) and the crystallographic water molecules were excluded prior to the energy minimization. The protein structure was then prepared using protein preparation wizard workflow as follows: adding hydrogen, assigning partial charges using OPLS-2005 force field and incorporating protonation states. The minimized structure was further used for screening and docking studies. The scaling factor of protein van der Waals radii for the receptor grid generation was set as 0.8 Å. Extra Precision (XP) method implemented in glide module was applied for the screening process, and the minimized compounds were docked to the grid volume. Based on the glide score, compounds were filtered and one of the top scored compounds NDGA was selected for the in vitro analysis. The literature survey also indicated that the compound is very promising for further study.

Determination of AChE inhibitory profile of the compound

Enzyme assays were carried out in a 96-well microtiter plate using AMPLITE™ AChE assay kit. The assay protocol was based on Ellman's method [26]. The electric eel AChE (EC 3.1.1.7) was used for the study since it is structurally similar to the nerve and muscle AChE of vertebrates [27, 28]. AChE solution at 1.37 μM concentration was prepared in double distilled water containing 0.1 % bovine serum albumin (BSA). Acetylthiocholine and Ellman's reagent [5, 5′-dithiobis-(2-nitrobenzoic acid) or (DTNB)] were used as the substrate and chromogenic compounds, respectively. Acetylthiocholine reaction mixture was prepared by adding 250 μl of each DTNB and acetylthiocholine stock solutions to 4.5 ml assay buffer (pH 7.4). The activity of the enzyme was assayed by mixing 25 μl AChE, 25 μl water and 50 μl acetylthiocholine reaction mixture. The optical density at a wave length of 415 nm was measured at intervals of 5 min, and a graph of optical densities (OD) versus time was plotted. NDGA (purchased from Sigma Aldrich, Bangalore, India) solutions with different concentrations (33, 66, 99 and 132 μM) were prepared in 0.1 % dimethylsulfoxide (DMSO). The enzyme was incubated with 25 μl of the NDGA solutions for 30 min and the assays were repeated as given above in order to test whether the compound can inhibit enzyme activity. It was also confirmed that DMSO has no inhibitory effect on AChE activity. For each NDGA concentration, an enzyme reaction was carried out and the OD was plotted against time. From the graph, the relative enzyme activity at each NDGA concentration was calculated. It was plotted against the concentrations of NDGA and IC_{50} values were calculated from the graph.

AChE assays were also carried out with different substrate concentrations (200, 400, 600, 800, 1000 and 1200 μM). The experiment was repeated using the enzyme incubated with 66 μM NDGA. Lineweaver-Burk plots (LB-plot) were drawn and the mode of inhibition of NDGA was determined. Kinetic parameters such as K_m and V_{max} were calculated from the LB-plot.

ADME prediction

A set of chemical descriptors relevant to the drug-likeness of all compounds was computed using QikProp module of the Schrödinger program. This predicts physically significant descriptors and pharmaceutically relevant properties of organic molecules. QikProp also provides a comparison between the properties of a particular compound with those of known drugs. Minimized ligands were given as the input for ADME prediction. The acceptability of the compound as a drug based on Lipinski's rule of five [29] was also estimated from the results.

Designing, induced-fit docking and free energy calculation

Drugs used for neurological treatments are generally CNS-active compounds. In order to improve the ADME profile, the structure of the NDGA was modified. All modified structures were drawn using Chemsketch program (ACDLABS 11.0, http://www.acdlabs.com/resources/freeware/chemsketch/) and energies were optimized using LigPrep module. Their physico-chemical properties were further predicted using QikProp and the distribution coefficient (LogD) was calculated using the Marvin sketch facility in the Chemaxon program.

To study ligand binding, the dynamic nature of biomolecules should be taken into consideration. The induced fit docking (IFD) approach is one of the feasible tools that considers flexibility of both protein and ligands. NDGA and its derivatives (which satisfied all properties) were subjected to IFD analysis. Initially, each ligand was docked to the protein using a softened potential. The resultant top 20 poses per ligand were then used to sample the protein plasticity using the prime program in the Schrödinger suite. Protein residues that are within 5 Å of the docked ligands were subjected to conformational flexibility. The flexible ligand was then redocked and the resultant poses were taken for further analysis.

The binding free energies of the promising ligands were calculated using the Prime MM-GBSA method. This method
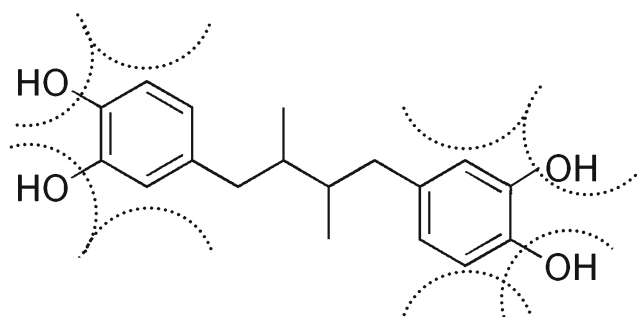

Fig. 2 Relative activity of Acetylcholinesterase (AChE) plotted against different concentration of NDGA. The absolute IC_{50} value was calculated from the graph

combines molecular mechanics energies (E_{MM}), surface generalized born solvation model for polar solvation (G_{SGB}), and a nonpolar solvation term (G_{NP}) in order to calculate the total free energy of binding between the protein and the ligand. The term G_{NP} includes nonpolar solvent accessible surface area and van der Waals interactions. The binding free energy was calculated using the following equation.

$$\Delta G_{Bind} = G_{Complex} - \left(G_{protein} + G_{Ligand} \right)$$

Where,

$$G = E_{MM} + G_{SGB} + G_{NP}$$

Fig. 1 Structure of NDGA {nordihydroguaiaretic acid; 4-[4-(3,4-dihydroxyphenyl)-2,3-dimethylbutyl]benzene-1,2-diol)} and the functional groups that have been modified
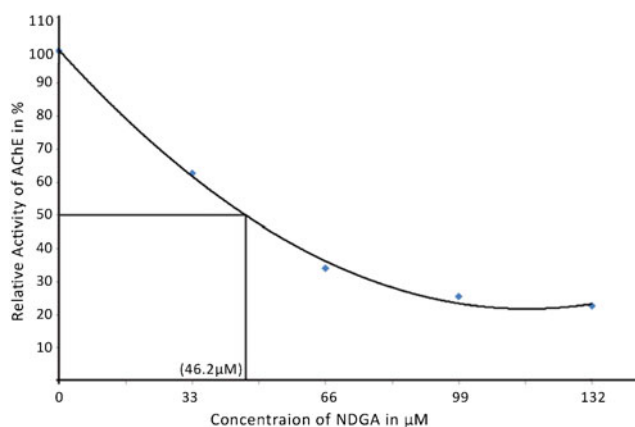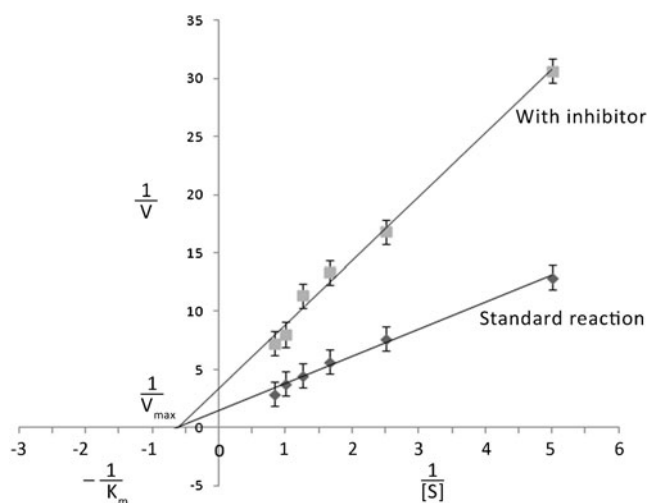

Fig. 3 Lineweaver-Burk plot of native AChE and the enzyme inhibited with NDGA. The values are averages of three independent measurements ± SD

Table 1 Properties relevant to blood brain barrier (BBB) penetration and central nervous system (CNS) activity for NDGA {nordihydroguaiaretic acid; 4-[4-(3,4-dihydroxyphenyl)-2,3-dimethylbutyl]benzene-1,2-diol)} and another 45 designed compounds predicted using the QikProp program. *HBD* Hydrogen bond donors, *HBA* hydrogen bond acceptors, *Mol_wt* molecular weight, *PSA* polar surface area

Molecule	Rotor	CNS	QPlog BB	Mol_wt	HBD	HBA	QPlogPo/w	No of N &O	PSA	LogD
NDGA	8	−2	−1.91	302	4	3	2.60	4	88	4.70
NDGA-D1	8	1	0.12	325	1	2.75	5.01	2	24	4.06
NDGA-D2	8	1	−0.11	325	1	2.75	5.02	2	28	4.11
NDGA-D3	9	1	−0.22	325	1	2.75	5.09	2	29	4.02
NDGA-D4	9	1	−0.17	340	1	2.75	5.51	2	27	4.18
NDGA-D5	9	1	−0.27	354	0	4	5.02	3	41	4.94
NDGA-D6	9	2	0.73	352	0	4	5.05	2	10	2.32
NDGA-D7	7	1	0.43	336	1	1.5	6.3	1	13	4.07
NDGA-D8	8	1	0.03	368	1	4.45	4.88	3	36	3.71
NDGA-D9	8	1	0.04	368	1	4.45	4.83	3	37	3.76
NDGA-D10	8	1	0.06	367	2	4.25	4.18	3	42	1.41
NDGA-D11	7	2	0.55	351	1	3.5	4.89	2	22	1.67
NDGA-D12	7	2	0.55	365	1	3.5	4.96	2	21	2.14
NDGA-D13	8	1	0.21	367	2	4.25	4.25	3	42	1.47
NDGA-D14	8	1	0.01	369	1	4.25	5.01	4	36	2.55
NDGA-D15	9	1	0.39	383	1	5	4.50	4	36	3.02
NDGA-D16	8	2	0.47	367	1	4.25	4.76	3	29	2.19
NDGA-D17	9	1	−0.03	366	2	4.25	4.29	3	44	1.80
NDGA-D18	9	1	−0.10	399	2	4	5.09	3	43	4.30
NDGA-D19	7	1	−0.17	338	1	2.75	5.57	2	28	3.90
NDGA-D20	8	1	−0.64	365	1	4	5.36	3	57	3.74
NDGA-D21	8	1	0.06	381	1	3.75	6.22	3	28	4.00
NDGA-D22	9	1	0.19	395	1	4.75	5.50	3	32	2.15
NDGA-D23	9	1	0.17	381	1	4.75	4.79	3	32	3.81
NDGA-D24	8	1	−0.57	381	1	5.75	3.78	4	57	4.13
NDGA-D25	8	2	0.50	365	1	3.5	5.2	2	21	1.93
NDGA-D26	9	1	−0.19	381	2	4.25	4.34	3	45	1.63
NDGA-D27	9	1	−0.15	381	2	4.25	4.47	3	44	1.64
NDGA-D28	8	1	0.12	367	0	4.75	4.81	4	36	4.20
NDGA-D29	8	2	0.48	381	1	3.75	5.03	3	27	4.2
NDGA-D30	8	1	0.04	352	2	3.75	4.12	3	42	3.43
NDGA-D31	9	1	0.08	396	2	5.75	3.93	4	45	3.42
NDGA-D32	8	1	−0.68	354	2	3.5	4.28	3	51	3.69
NDGA-D33	8	1	0.05	363	1	3.75	5.06	3	37	4.12
NDGA-D34	9	1	−0.52	379	2	4.5	4.55	4	58	3.72
NDGA-D35	6	1	0.43	378	2	3.5	4.77	3	35	4.72
NDGA-D36	7	1	0.33	392	2	4.5	4.19	3	37	2.55
NDGA-D37	5	2	0.84	335	1	2.5	4.84	2	20	4.60
NDGA-D38	6	1	0.24	351	2	3.25	4.03	3	43	4.30
NDGA-D39	6	1	0.31	365	2	3.25	4.40	3	42	4.82
NDGA-D40	6	2	0.78	365	1	3.25	4.94	3	29	4.45
NDGA-D41	7	2	0.71	395	1	4	5.07	4	35	4.29
NDGA-D42	8	1	0.37	436	2	5.25	4.67	4	45	3.62
NDGA-D43	7	2	0.66	420	1	4.5	5.28	3	25	3.54
NDGA-D44	8	1	0.38	436	1	5.75	4.72	4	34	4.10
NDGA-D45	8	2	0.51	435	1	5.75	4.78	4	35	4.35

Table 2 Physico-chemical parameters predicted for NDGA and its derivatives using QikProp. *SASA* Solvent accessible surface area, *FOSA* hydrophobic component of the SASA, *HOA* human oral absorption

Molecule	Volume	SASA	FOSA	QPPCaco	QPPMDCK	QPlogKhsa	HOA	% HOA	G Score
NDGA	1,022	585	168	116	49	0.16	3	80	−10.90
NDGA-D1	1,203	668	371	1,113	612	1.03	3	100	−14.40
NDGA-D2	1,212	678	377	701	373	1.05	3	95	−10.37
NDGA-D3	1,228	694	372	644	340	1.05	3	95	−12.71
NDGA-D4	1,274	710	403	715	382	1.18	3	100	−16.24
NDGA-D5	1,317	748	381	638	337	0.9	3	94	−13.43
NDGA-D6	1,358	756	530	513	294	1.10	3	94	−14.17
NDGA-D7	1,267	707	399	1979	1,144	1.49	1	100	−11.56
NDGA-D8	1,289	705	495	944	514	0.92	3	100	−14.53
NDGA-D9	1,290	707	496	808	534	0.92	3	100	−16.14
NDGA-D10	1,317	730	485	112	57	0.95	3	88	−14.68
NDGA-D11	1,298	721	489	273	149	1.18	3	100	−13.17
NDGA-D12	1,344	740	544	275	150	1.30	3	88	−15.38
NDGA-D13	1,310	723	480	150	78	0.93	3	91	−13.40
NDGA-D14	1,296	719	498	909	504	0.97	3	96	−11.64
NDGA-D15	1,344	737	512	249	135	0.91	3	96	−14.22
NDGA-D16	1,335	741	537	265	144	1.08	3	100	−14.50
NDGA-D17	1,331	744	479	110	56	0.94	3	87	−14.40
NDGA-D18	1,347	739	471	638	650	1.03	3	95	−13.09
NDGA-D19	1,306	672	465	657	347	1.3	1	100	−13.01
NDGA-D20	1,382	798	482	310	154	1.25	1	90	−12.36
NDGA-D21	1,453	837	614	940	512	1.50	1	100	−15.26
NDGA-D22	1,511	863	637	202	108	1.40	1	88	−14.48
NDGA-D23	1,383	765	466	166	87	1.06	3	95	−14.57
NDGA-D24	1,347	752	416	180	148	0.47	3	89	−13.81
NDGA-D25	1,351	742	486	280	152	1.28	3	88	−13.16
NDGA-D26	1,359	741	467	75	37	1.02	3	86	−13.84
NDGA-D27	1,374	755	486	85	42	1.06	3	88	−12.41
NDGA-D28	1,275	703	424	1139	623	0.71	3	100	−12.64
NDGA-D29	1,375	755	554	269	147	1.29	3	88	−15.97
NDGA-D30	1,265	708	384	105	53	0.90	3	87	−13.50
NDGA-D31	1,440	806	547	37	19	0.94	2	78	−16.27
NDGA-D32	1,233	680	348	193	93	0.87	3	93	−12.57
NDGA-D33	1,281	712	340	819	541	1.03	3	97	−13.27
NDGA-D34	1,297	719	334	347	175	0.81	3	100	−14.25
NDGA-D35	1,335	734	513	188	99	1.22	3	96	−15.74
NDGA-D36	1,390	759	508	44	22	1.14	3	81	−14.97
NDGA-D37	1,195	662	374	381	213	1.18	3	100	−10.90
NDGA-D38	1,217	673	374	115	58	0.95	3	87	−12.34
NDGA-D39	1,274	702	457	142	73	1.10	3	91	−15.41
NDGA-D40	1,269	699	467	381	213	1.19	3	100	−12.15
NDGA-D41	1,349	736	550	380	213.	1.21	3	90	−17.55
NDGA-D42	1,518	815	659	55	29	1.30	3	85	−18.20
NDGA-D43	1,509	815	668	88	48	1.55	2	80	−12.57
NDGA-D44	1,522	819	618	57	30	1.27	1	86	−15.85
NDGA-D45	1,516	813	612	73	39	1.26	3	88	−17.14

Table 3 Molecular structures and IUPAC names of NDGA and its derivatives

Name of the compound	Chemical structure	IUAC Name
NDGA- D1		4-(3-benzyl-2-methylbutyl)-2-[(1S)-1-(dimethylamino)ethyl]phenol
NDGA- D2		4-[3-({4-[(1R)-1-(dimethylamino)ethyl]phenyl}methyl)-2-methylbutyl]phenol
NDGA- D3		3-[3-({4-[2-(dimethylamino)ethyl]phenyl}methyl)-2-methylbutyl]phenol
NDGA- D4		3-[3-({3-[(2R)-1-(dimethylamino)propan-2-yl]phenyl}methyl)-2-methylbutyl]phenol
NDGA-D5		2 -(dimethylamino)ethyl 4-(2,3-dimethyl-4-phenylbutyl)benzoate
NDGA- D6		2 -(dimethylamino)ethyl 4-(2,3-dimethyl-4-phenylbutyl)benzoate
NDGA-7		2-{[4-(2,3-dimethyl-4-phenylbutyl)phenyl]methyl}piperidine

Results and discussion

Among 216 compounds taken for screening, 178 were docked successfully to the active site of hAChE. The glide score for these ligands after XP docking ranged from −3.67 to −10.71 kcal/mol. NDGA was one of the top scoring compounds, with a glide score of −9.19 kcal/mol and was taken for further analysis. NDGA possesses anti-oxidative and

neuroprotective properties. It also has an anti aggregation effect towards Aβ peptide accumulation. The glide score of NDGA was also comparable to the already reported AChE inhibitors like donepezil, tacrine, galanthamine, rivastigmine, physostigmine and huperzine. Their respective glide score after XP docking were −10.34, -8.09, −9.02, −6.49, −7.44 and −7.92 kcal/mol. The structure of NDGA is shown in Fig. 1.

Table 3 (continued)

Name of the compound	Chemical structure	IUAC Name
NDGA-D8		2-(dimethylamino)ethyl 4-(2,3-dimethyl-4-phenylbutyl)benzoate
NDGA-D9		6-[3-({4-[(1S)-1-(dimethylamino)ethyl]phenyl}methyl)-2-methylbutyl]-1,3-dihydro-2-benzofuran-4-ol
NDGA-D10		5-[4-(2,3-dihydro-1H-isoindol-5-yl)-2,3-dimethylbutyl]-2-[(1S)-1-(dimethylamino)ethyl]phenol
NDGA-D11		[(1S)-1-{4-[4-(2,3-dihydro-1H-isoindol-5-yl)-2,3-dimethylbutyl]phenyl}ethyl]dimethylamine
NDGA-D12		[(1S)-1-{4-[4-(2,3-dihydro-1H-isoindol-5-yl)-2,3-dimethylbutyl]-2-methylphenyl}ethyl]dimethylamine
NDGA-13		5-[3-({4-[(1S)-1-(dimethylamino)ethyl]phenyl}methyl)-2-methylbutyl]-2,3-dihydro-1H-isoindol-4-ol
NDGA-D14		{5-[4-(2,3-dihydro-1H-isoindol-5-yl)2,3-dimethylbutyl]-2-methoxyphenoxy}dimethylamine
NDGA-D15		{5-[4-(2,3-dihydro-1H-isoindol-5-yl)-2,3-dimethylbutyl]-2-methoxyphenoxymethyl}dimethylamine

Table 3 (continued)

Name of the compound	Chemical structure	IUAC Name
NDGA-D16		({5-[4-(2,3-dihydro-1H-isoindol-5-yl)-2,3-dimethylbutyl]-2-methoxyphenyl}methyl)dimethylamine
NDGA-D17		5-[4-(2,3-dihydro-1H-isoindol-5-yl)2,3-dimethylbutyl]-2-[2-(dimethylamino)ethyl]phenol
NDGA-D18		5-[3-({4-[(1S)-1-(dimethylamino)ethyl]-3-hydroxyphenyl}methyl)-2-methylbutyl]-1,3-dihydro-2-benzothiophen-4-ol
NDGA-19		4-{4-[2-(dimethylamino)-2,3-dihydro-1H-inden-5-yl]-2,3-dimethylbutyl}phenol
NDGA-20		4-{4-[2-(dimethylamino)-2,3-dihydro-1H-inden-5-yl]-2,3-dimethylbutyl}phenyl carboximidate
NDGA-21		2-(dimethylamino)-5-{4-[2-(dimethylamino)-2,3-dihydro-1H-inden-5-yl]-2,3-dimethylbutyl}phenol

The IC$_{50}$ value obtained for NDGA on AChE was 46.2 μM (Fig. 2). The mode of inhibition of NDGA and its effect on both K_m and V_{max} values was determined from the LB-plot (Fig. 3). The K_m value obtained for the enzyme was 0.91 μM irrespective of whether or not it was treated with NDGA. A decrease in the V_{max} from 0.71 to

Table 3 (continued)
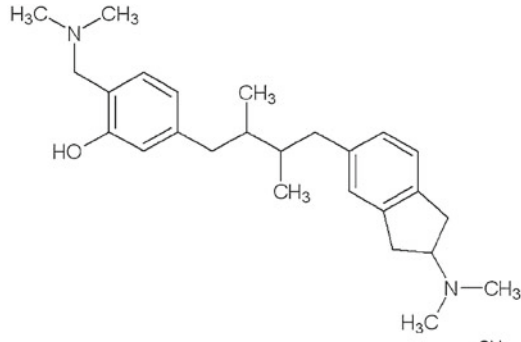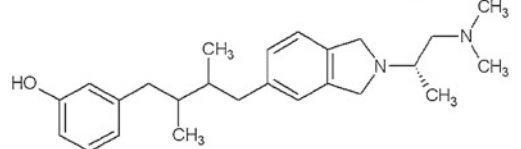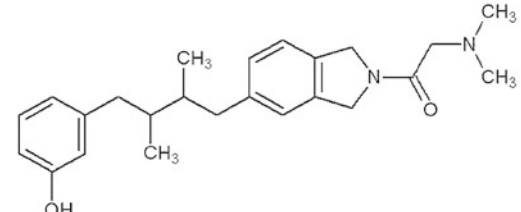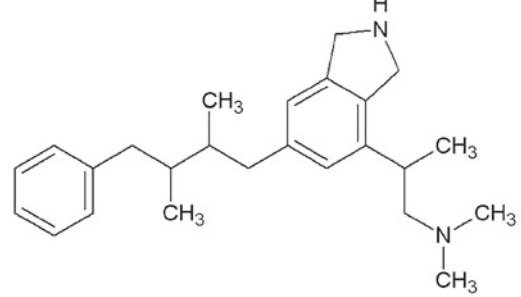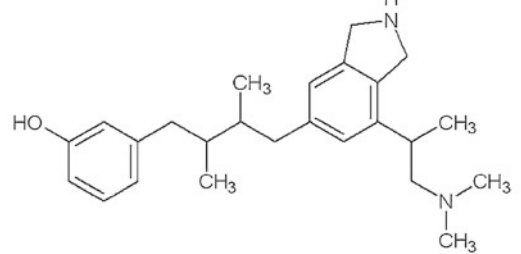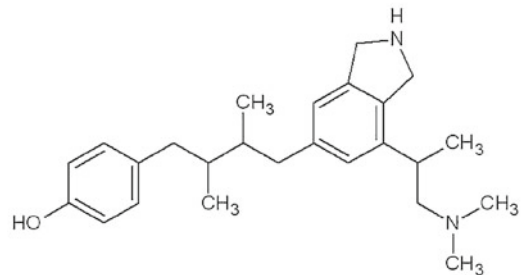
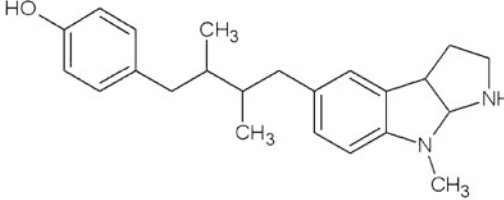| Name of the compound	Chemical structure	IUAC Name
NDGA-22		5-{4-[2-(dimethylamino)-2,3-dihydro-1H-inden-5-yl]-2,3-dimethylbutyl}-2-[(dimethylamino)methyl]phenol
NDGA-23		3-(4-{2-[(2S)-1- (dimethylamino)propan-2-yl]-2,3-dihydro-1H-isoindol-5-yl}- 2,3-dimethylbutyl)phenol
NDGA-D24		2-(dimethylamino)-1-(5-{3-[(3-hydroxyphenyl)methyl] -2- methylbutyl}-2,3 -dihydro-1H-isoindol-2-yl)ethan-1one
NDGA-25		{2-[6-(3-benzyl-2-methylbutyl)-2,3-dihydro-1H-isoindol-4-yl]propyl}dimethylamine
NDGA-D26		3-(4-{7-[1-(dimethylamino)propan-2-yl]-2,3-dihydro-1H-isoindol-5-yl}-2,3-dimethylbutyl)phenol
NDGA-D27		4-(4-{7-[1-(dimethylamino)propan-2-yl]-2,3-dihydro-1H-isoindol-5-yl}-2,3-dimethylbutyl)phenol
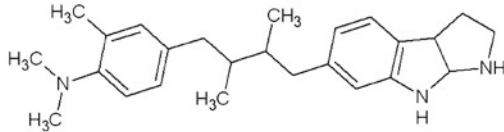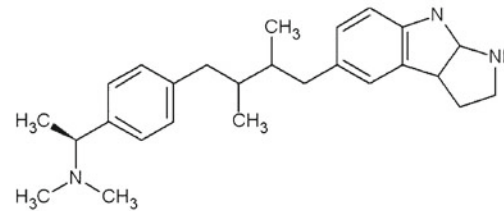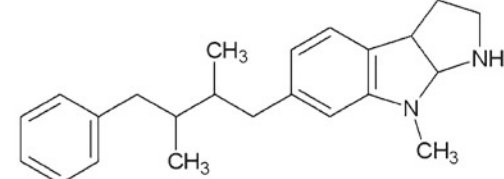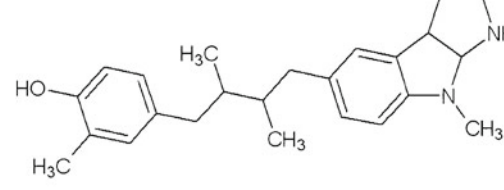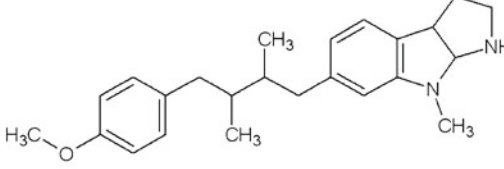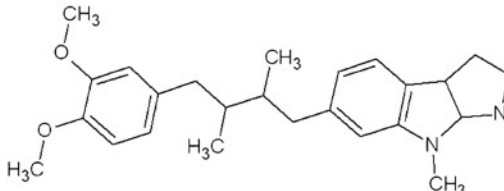
Table 3 (continued)

Name of the compound	Chemical structure	IUAC Name
NDGA-D28		({4-[4-(1,3-benzoxazol-6-yl)-2,3-dimethylbutyl]-2-methoxyphenyl}methyl)dimethylamine
NDGA-D29		4-[2,3-dimethyl-4-(1-methyl-2,3-dihydro-1H-indol-5-yl)butyl]-2-[(1S)-1-(dimethylamino)ethyl]phenol
NDGA-D30		4-(4-{2-[(dimethylamino)methyl]-2,3-dihydro-1H-indol-5-yl}-2,3-dimethylbutyl)phenol
NDGA-D31		4-{4-[2-(dimethylamino)-2,3-dihydro-1H-indol-5-yl]-2,3-dimethylbutyl}-2-[(dimethylamino)methyl]phenol
NDGA-D32		2-(dimethylamino)-7-{3-[(4-hydroxyphenyl)methyl]-2-methylbutyl}-2,3-dihydro-1H-inden-5-ol
NDGA-D33		6 -(4-{4- [(dimethylamino)methyl]phenyl}-2,3-dimethylbutyl)quinolin-5-ol
NDGA-D34		6-(4-{4-[(dimethylamino)methyl]-3-hydroxyphenyl}-2,3-dimethylbutyl)quinolin-5-ol

0.30 μM min^{-1} mg^{-1} was observed when the enzyme treated with NDGA. The results revealed that NDGA is a noncompetitive inhibitor as it decreases the V_{max} value without affecting the K_m value.

Table 3 (continued)

Name of the compound	Chemical structure	IUAC Name
NDGA-D35		4-(4-{1H,2H,3H,3aH,8H,8aH-pyrrolo[2,3-b]indol-6-yl}-2,3-dimethylbutyl)-N,N,2-trimethylaniline
NDGA-D36		[(1S)-1-[4-(4-{1H,2H,3H,3aH,8H,8aH-pyrrolo[2,3-b]indol-5-yl}-2,3-dimethylbutyl)phenyl]ethyl]dimethylamine
NDGA-D37		6-(3-benzyl-2-methylbutyl)-8-methyl-1H,2H,3H,3aH,8H,8aH-pyrrolo[2,3-b]indole
NDGA-D38		4-(2,3-dimethyl-4-{8-methyl-1H,2H,3H,3aH,8H,8aH-pyrrolo[2,3-b]indol-5-yl}butyl)phenol
NDGA-D39		4-(2,3-dimethyl-4-{8-methyl-1H,2H,3H,3aH,8H,8aH-pyrrolo[2,3-b]indol-5-yl}butyl)-2-methylphenol
NDGA-D40		6-{3-[(4-methoxyphenyl)methyl]-2-methylbutyl}-8-methyl-1H,2H,3H,3aH,8H,8aH-pyrrolo[2,3-b]indole
NDGA-D41		6-{3-[(3,4-dimethoxyphenyl)methyl]-2-methylbutyl}-8-methyl-1H,2H,3H,3aH,8H,8aH-pyrrolo[2,3-b]indole

In silico predictions have been used for determining ADME parameters such as absorption, distribution and metabolism [30]. NDGA showed poor BBB permeability and CNS activity. The physico-chemical parameters of NDGA are given in Tables 1 and 2. Properties such as molecular weight (mol_wt), hydrogen bond acceptors (HBA), rotatable bonds (rotor), molecular volume (volume), solvent accessible surface area (SASA), LogP value (QPlogPo/w) and binding to the human

Table 3 (continued)

Name of the compound	Chemical structure	IUAC Name
NDGA-D42		5-[3-({3-[(1S)-1-(dimethylamino)ethyl]-5-methylphenyl}methyl)-2-methylbutyl]-8-methyl-1H,2H,3H,3aH,8H,8aH-pyrrolo[2,3-b]indol-4-ol
NDGA-D43		[(1S)-1-[3-(2,3-dimethyl-4-{8-methyl-1H,2H,3H,3aH,8H,8aH-pyrrolo[2,3-b]indol-5-yl}butyl)-5-methylphenyl]ethyl]dimethylamine
NDGA-D44		4-(4-{1,8-dimethyl-1H,2H,3H,3aH,8H,8aH-pyrrolo[2,3-b]indol -5-yl}-2,3-dimethylbutyl)-2-[(1S)-1-(dimethylamino)ethyl]phenol
NDGA-D45		5-[3-({3-[(1S)-1-(dimethylamino)ethyl]phenyl}methyl)-2-methylbutyl]-1,8-dimethyl-1H,2H,3H,3aH,8H,8aH-pyrrolo[2,3-b]indol-4-ol

serum albumin (QPlogKhSa) were within the allowed range. The percentage of human oral absorption (HOA) for NDGA was also within the acceptable limit. An important physico-chemical property of a potential CNS drug is its ability to cross the BBB, which in turn depends on the lipophilicity of the drug. Most CNS-acting agents are lipophilic and can cross the BBB by passive diffusion [31]. The four hydroxyl groups on NDGA make it unsuitable for such penetration and hence CNS inactive. In order to improve BBB permeability and CNS activity, the structure of NDGA was modified as discussed below.

It has been reported that possession of a positive charge at pH 7–8 (usually due to the presence of tertiary nitrogen) tends to favor brain permeation [32]. Andrews et al. [33] reported that an aromatic ring-tertiary nitrogen pharmacophore enhances CNS activity. In order to increase the hydrophobicity, the number of electronegative atoms such as nitrogen and oxygen were limited to five. The hydroxyl groups of NDGA were modified accordingly and are shown in Fig. 1.

About 350 derivatives were designed through structural modification and their drug likeness was predicted using the QikProp program. Of these, only 99 derivatives exhibited favorable BBB penetration value (QPLogBB) and CNS activity; the rest were excluded from further studies. In order to standardize the properties of CNS acting drugs, 170 known CNS acting agents were collected [34] and their physico-chemical properties analyzed. CNS activity scale

and QPLogBB penetration values for these compounds were between 1–2 and −0.11–1.12 respectively. The preferred values for the parameters such as mol_wt ≤ 450 Da; rotor ≤ 9; HBD ≤ 3; HBA ≤ 7; LogP < 5; PSA < 60–70 Å^2; and number of H-bonds <8 have already been reported [35].

Amine and aromatic moieties are known to be important for BBB penetration and CNS activity [36]. The analysis confirmed that all 99 derivatives contain these moieties in their structure. These derivatives were also found to be basic or neutral in character. The mol_wt of almost all designed compounds was below 400 Da and the number of hydrogen bond donors and acceptors were within the allowed limits. The PSA value is a major determinant of passive permeability [37] and BBB penetration will be optimal when PSA is <65 Å^2. It was also found that CNS activity is directly proportional to the ratio between hydrophobic and hydrophilic surface areas.

Usually, the parameter that describes lipophilicity is LogP. It was reported that 95 % of all drugs are ionizable at various pH [38]. Sanjivanjit et al. [39] reported that, instead of using LogP, it is more appropriate to use LogD for representing lipophilicity because it reflects the true behavior of ionizable compounds. Therefore, LogD was taken for filtering derivatives in the present analysis. Only ligands with LogD ≤5 at pH 7.4 were taken for further study. It is already described that the CNS-active compounds in general have larger LogP (more lipophilic) than other biologically active molecules [36]. Based on the number of rotatable bonds (≤9) and LogD values (≤5), the derivatives were filtered to 45 and are named NDGA-D1 to D45 (Table 3). The properties calculated for these 45 ligands are shown in Tables 1 and 2. NDGA and these 45 derivatives were then subjected to IFD analysis to investigate the atomic level interaction with AChE.

Numerous in vitro models of the BBB have been established, including kidney cells (Mandin-Darby canine kidney, MDCK) and intestinal epithelial cells (Caco-2 cell lines) [40–42]. MDCK cells offered the best model in terms of predicting BBB penetration based on micro dialysis data [43]. Alavijeh et al. [31] reported that the passive permeability determined in MDCK cell is 475 nm/s. From the in silico prediction of Caco and MDCK permeability values of known CNS-acting agents, it is also confirmed that ligands should have higher Caco (QPPCaco) and MDCK (QPPMDCK) permeability values (> 500 nm/s).

All compounds that had Caco and MDCK permeability values less than 500 nm/s were omitted from the binding analysis. Even though the glide score (expressed in kcal/mol) of the ligands such as D42 (−18.20), D45 (−17.14), D41 (−17.55), D31 (−16.27), D44 (−15.85), D35 (−15.74), D39 (−15.41) and D12 (−15.38) were high, they were excluded because of low Caco and MDCK permeability. Derivatives such as NDGA-D1, D7, D8, D9, D14, D18, D21, D28 and D33 possess all the required parameters for successful CNS-acting compounds. The ranges of Caco and

MDCK permeability values obtained were 638–1,174 and 514–1,144 nm/s, respectively.

Finally, the binding pattern of NDGA and these nine derivatives at the active site of hAChE was analyzed thoroughly. The binding free energy of NDGA and other selected derivatives is shown in Table 4. The binding mode of NDGA and these ligands at the active site of hAChE is displayed in Fig. 4.

The glide score of NDGA after IFD analysis was −10.91 kcal/mol. An important structural feature of NDGA is the presence of two catechol moieties; these moieties are involved mainly in the binding of NDGA at the active site of hAChE. One of the catechol moieties was engaged in hydrogen bonding with Phe295 through its hydroxyl group. Another catechol moiety interacts with Trp86 through its π electrons and thereby forms a stacking interaction. Also both hydroxyl groups were involved in bifurcated hydrogen bonding with carbonyl oxygen atom of His447. Interactions formed with His447 (an active site residue) and Phe295 (a PAS residue) reveals that the binding is extending from active site to PAS. The binding is also stabilized by hydrophobic contacts with residues lining the PAS such as Tyr124, Trp286, Phe295, Val294, Phe297, Tyr337, Phe338 and Tyr341. The interactions with PAS residues may prevent Aβ binding to this site and formation of the AChE-Aβ complex.

The glide scores obtained for NDGA-D1, D7, D8, D9, D14, D18, D21, D28 and D33 were −14.40, −11.56, −14.53, −16.14, −11.64, −13.09, −15.26, −12.64 and −13.27 kcal/mol respectively. As expected, binding is stabilized mainly by various stacking interactions, hydrogen bonds and hydrophobic

Table 4 Glide score and binding free energy of NDGA and its derivatives selected based on acceptable Caco and MDCK values along with five known AChE inhibitors

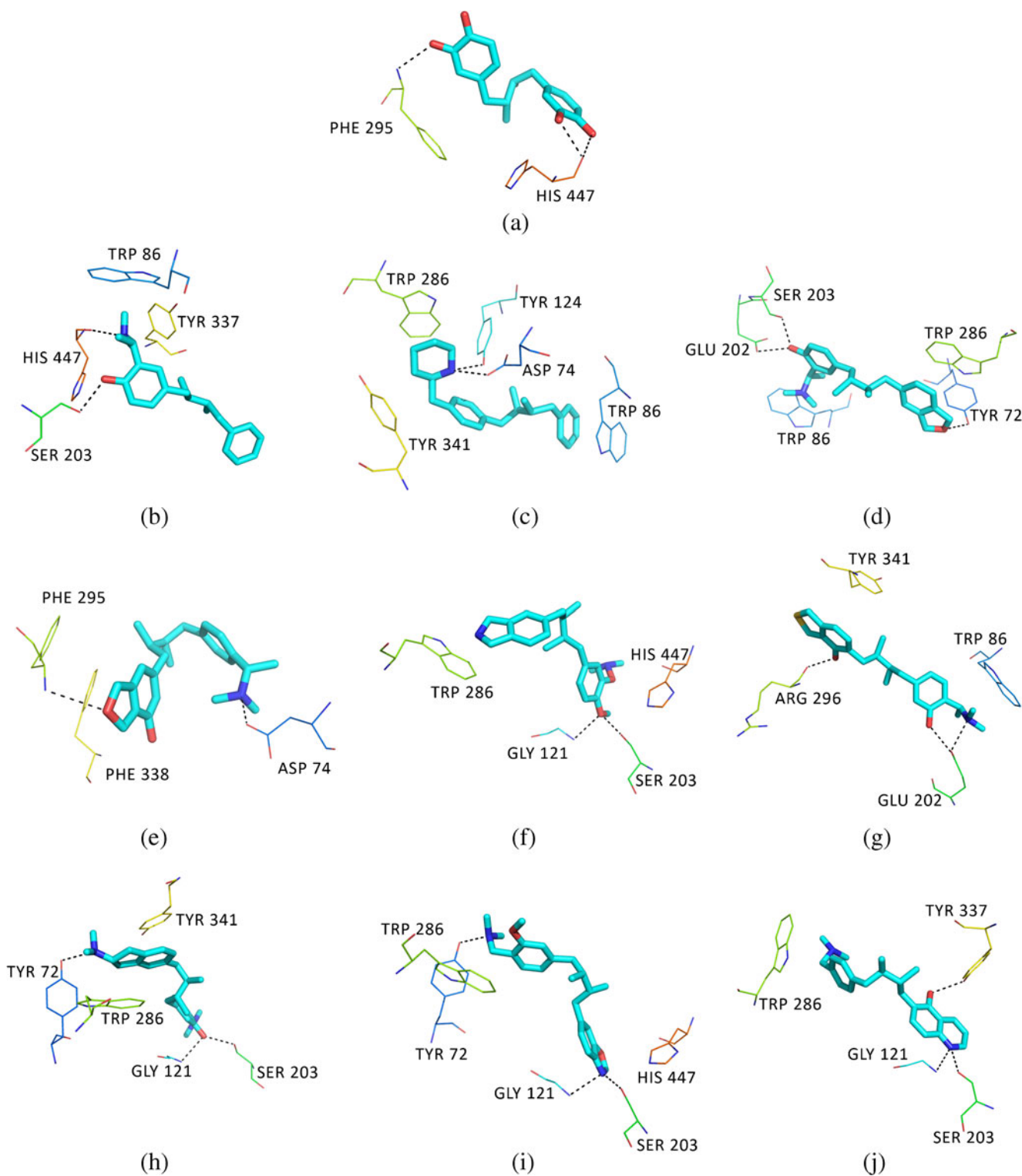| No	Ligand name	Glide score (kcal/mol)	ΔG (kcal/mol)
1	NDGA	−10.90	−34.99
2	NDGA D1	−14.40	−53.56
3	NDGA-D7	−11.56	−50.74
4	NDGA-D8	−14.53	−52.45
5	NDGA-D9	−16.14	−70.28
6	NDGA-D14	−11.64	−46.97
7	NDGA-D18	−13.09	−63.55
8	NDGA-D21	−15.26	−55.40
9	NDGA-D28	−12.64	−49.19
10	NDGA-D33	−13.27	−58.05
11	Donepezil	−11.07	−58.29
12	Tacrine	−8.08	−20.10
13	Rivastigmine	−10.78	−34.55
14	Physostigmine	−9.90	−59.99
15	Memantine	−9.08	−45.03

Fig. 4 Mode of binding of NDGA and selected derivatives in the active site of AChE. Hydrogen bonds are shown by *dotted lines*. **a** NDGA, **b** NDGA–D1, **c** NDGA–D7, **d** NDGA–D8, **e** NDGA–D9, **f** NDGA–D14, **g** NDGA–D18, **h** NDGA–D21, **i** NDGA–D28, **j** NDGA–D31

interactions. All ligands exhibited either cation–π or π–π interactions with any of these residues such as Trp86, Trp286, His447, Phe338, Tyr337 and Tyr341. An important catalytic residue, Ser203, was found to form hydrogen bonds with

ligands such as NDGA-D1, D8, D14, D21, D28 and D31. NDGA-D1 also forms hydrogen bonds with the other catalytically important residue His447. The formation of hydrogen bonds with Ser203 and His447 seems to be very crucial; it very

likely masks these residues and prevents them from taking part in catalysis. The binding of NDGA D7, D9, D8 and D18 are also characterized by salt bridges with Asp74 and Glu202, respectively. NDGA-D8 and D28 have hydrogen bonds with Tyr72. The ligands NDGA-D14 and D28 also showed hydrogen bonds with Gly121, one of the residues that forms the oxyanion hole. The binding mode of all ligands was found to extend from the active site to PAS.

The present study leads to the conclusion that selected NDGA derivatives will have a better ADME and AChE inhibitory profile for use as anti-AD agents.

Conclusions

Although many potential compounds have been reported against AChE, there is still no cure for AD. Therefore it is essential to identify new anti AD drug candidates. Polyphenolic compounds are reported to possess a variety of desired biological activities for human health. In the present work, we have carried out a preliminary screening of chemically diverse secondary metabolites against AChE. The top-scoring compound, NDGA, was subjected to enzyme kinetic studies. In addition, the physico-chemical properties of NDGA were modified according to the attributes of a successful CNS-acting agent. CNS drugs are generally more lipophilic, less flexible and have lower molecular weight than drugs used for other therapeutic purposes. IFD analysis showed better binding affinity for the designed ligands. Hydrogen bonding and π–π interactions are observed as important stabilizing factors in the binding of these ligands to AChE. We have designed some NDGA derivatives as AChE inhibitors with good ADME profile for further investigation and experimental validation. Molecular docking, designing and ADME predictions can be important primary steps toward the identification of novel drug candidates for AD.

References

1. Selkoe DJ, Schenk D (2003) Alzheimer's disease: molecular understanding predicts amyloid-based therapeutics. Annu Rev Pharmacol Toxicol 43:545–584
2. Schliebs R (2005) Basal forebrain cholinergic dysfunction in Alzheimer's disease–interrelationship with beta-amyloid, inflammation and neurotrophin signaling. Neurochem Res 30:895–908
3. Goedert M, Spillantini MG (2006) A century of Alzheimer's disease. Science 314:777–781
4. Luttmann E, Linnemann E, Fels G (2002) Galantamine as bisfunctional ligand for the acetylcholinesterase. J Mol Model 8:208–216
5. Schrattenholz A, Pereira EF, Roth U, Weber KH, Albuquerque EX, Maelicke A (1996) Agonist responses of neuronal nicotinic acetylcholine receptors are potentiated by a novel class of allosterically acting ligands. Mol Pharmacol 49:1–6
6. Coyle JT, Geerts H, Sorra K, Amatniek J (2007) Beyond in vitro data: a review of in vivo evidence regarding the allosteric potentiating effect of galantamine on nicotinic acetylcholine receptors in Alzheimer's neuropathology. J Alzheimers Dis 11:491–507
7. Reyes AE, Chacon MA, Dinamarca MC, Cerpa W, Morgan C, Inestrosa NC (2004) Acetylcholinesterase—Abeta complexes are more toxic than Abeta fibrils in rat hippocampus: effect on rat beta-amyloid aggregation, laminin expression, reactive astrocytosis, and neuronal cell loss. Am J Pathol 164:2163–2174
8. Castro A, Martinez A (2006) Targeting beta-amyloid pathogenesis through acetylcholinesterase inhibitors. Curr Pharm Des 12:4377–4387
9. Kasa P, Papp H, Kasa P Jr, Torok I (2000) Donepezil dose-dependently inhibits acetylcholinesterase activity in various areas and in the presynaptic cholinergic and the postsynaptic cholinoceptive enzyme-positive structures in the human and rat brain. Neuroscience 101:89–100
10. Kurz A (1998) The therapeutic potential of tacrine. J Neural Transm Suppl 54:295–299
11. Sugimoto H (2001) Donepezil hydrochloride: a treatment drug for Alzheimer's disease. Chem Rec 1(1):63–73
12. Zarotsky V, Sramek JJ, Cutler NR (2003) Galantamine hydrobromide: an agent for alzheimer's disease. Am J Health Syst Pharm 60:446–452
13. Jann MW (2000) Rivastigmine, a new- generation cholinesterase inhibitor for the treatment of Alzheimer's disease. Pharmacotherapy 20(1):1–12
14. Francis PT, Nordberg A, Arnold SE (2005) A preclinical view of cholinesterase inhibitors in neuroprotection: do they provide more than symptomatic benefits in Alzheimer's disease? Trends Pharmacol Sci 26:104–111
15. Wang YE, Yue DX, Tang XC (1986) Anticholinesterase activity of huperzine A. Acta pharmacol Sin 7:110–113
16. Barak D, Ordentlich A, Stein D, Yu QS, Greig NH, Shafferman A (2009) Accommodation of physostigmine and its analogs by acetylcholinesterase is dominated by hydrophobic interactions. Biochem J 417(1):213–222
17. Arteaga S, Andrade-Cetto A, Cardenas R (2005) *Larrea tridentate* (creosote bush) an abundant palnt of Mexican and US-american desert and its metabolite nordihydroguairetic acid. J Ethnopharmol 98(3):231–239
18. Oliveto EP (1972) Nordihydroguaiaretic acid. A naturally occurring antioxidant. Chem Ind 17:677–679
19. Noor R, Mittal S, Iqbal J (2002) Superoxide dismutase- applications and relevance to human diseases. Med Sci Monit 8:RA210–RA215
20. Guzman-Beltran S, Espada S, Orozco-Ibarra M, Pedraza-Chaverri J, Cuadrado A (2008) Nordihydroguaiaretic acid activates the antioxidant pathway Nrf2/HO-1 and protects cerebellargranule neurons against oxidative stress. Neurosci Lett 447:167–171
21. Goodman Y, Steiner MR, Steiner SM, Mattson MP (1994) Nordihydroguaiaretic acid protects hippocampal neurons against amyloid beta-peptide toxicity, and attenuates free radical and calcium accumulation. Brain Res 654:171–176
22. Rothman SM, Yamada KA, Lancaster N (1993) Nordihydroguaiaretic acid attenuates NMDA neurotoxicity—action beyond the receptor. Neuropharmacology 32:1279–1288

23. Boston-Howes W, Williams EO, Bogush A, Scolere M, Pasinelli P, Trotti D (2008) Nordihydroguaiaretic acid increases glutamate uptake in vitro and in vivo: therapeutic implications for amyotrophic lateral sclerosis. Exp Neurol 213:229–237

24. Shishido Y, Furushiro M, Hashimoto S, Yokokura T (2001) Effect of nordihydroguaiaretic acid on behavioral impairment and neuronal cell death after forebrain ischemia. Pharmacol Biochem Behav 69:469–474

25. Majumdar DK, Govil JN, Singh VK (2003) Recent progress in medicinal plants. Vol 8 Phytochemistry and Pharmacology. Studium, Houston, TX

26. Ellman GL, Courtney KD, Andres V Jr, Featherstone RM (1961) Biochem Pharmacol 7:88–95

27. Sussman JL, Harel M, Frolow F, Oefner C, Goldman A, Toker L, Silman I (1991) Science 253:872–879

28. Bon S, Vigny M, Massoulie J (1979) Asymmetric and globular forms of acetylcholinesterase in mammals and birds. Proc Natl Acad Sci USA 76:2546–2550

29. Lipinski CA, Lombardo F, Dominy BW, Feeney PJ (2001) Experimental and computational approaches to estimate solubility and permeability in drug discovery and development settings. Adv Drug Deliv Rev 46:3–26

30. Ekins S, Waller CL, Swann PW, Cruciani G, Wrighton SA, Wikel JH (2000) J Pharmacol Toxicol 44:251–272

31. Alavijeh MS, Chishty M, Qaiser MZ, Palmer AM (2005) Drug metabolism and pharmacokinetics, the blood-brain barrier, and central nervous system drug discovery. NeuroRx 2:554–571

32. Clark DE (2003) In silico prediction of blood–brain barrier permeation. Drug Discov Today 8:927–933

33. Lloyd EJ, Andrews PR (1986) A common structural model for central nervous system drugs and their receptors. J Med Chem 29:453–462

34. Lemke TL, Williams DA, Roche VF, Zito SW (2008), Foye's principles of medicinal chemistry. Wolters Kluwer/Lippincott Williams and Wilkins, Baltimore

35. Pajouhesh H, Lenz GR (2005) Medicinal chemical properties of successful central nervous system drugs. NeuroRx 2:541–553

36. Clark DE (1999) Rapid calculation of polar molecular surface area and its application to the prediction of transport phenomena. 2. Prediction of blood–brain barrier penetration. J Pharm Sci 88:815–821

37. Ajay, Bemis GW, Murcko MA (1999) Designing libraries with CNS activity. J Med Chem 42:4942–4951

38. Balon K, Riebesehl BU, Muller BW (1999) Determination of liposome partitioning of ionizable drugs by titration. J Pharm Sci 88:802–806

39. Bhal SK, Kassam K, Peirson IG, Pearl GM (2007) The rule of five revisited: applying log d in place of log p in drug-likeness filters. Mol Pharmaceut 4:556–560

40. Garberg P, Ball M, Borg N, Cecchelli R, Fenart L, Hurst RD, Lindmark T, Mabondzo A, Nilsson JE, Raub TJ, Stanimirovic D, Terasaki T, Oberg JO (2005) In vitro models for the blood–brain barrier. Toxicol In Vitro 19:299–334

41. Deli MA, Abraham CS, Kataoka Y, Niwa M (2005) Permeability studies on in vitro blood–brain barrier models: physiology, pathology, and pharmacology. Cell Mol Neurobiol 25:59–127

42. Reichel A, Begley DJ, Abbott NJ (2003) An overview of in vitro techniques for blood–brain barrier studies. Methods Mol Med 89:307–324

43. Doan KM, Humphreys JE, Webster LO, Wring SA, Shampine LJ, Serabjit-Singh CJ (2002) Passive permeability and P-glycoproteinmediated efflux differentiate central nervous system (CNS) and non-CNS marketed drugs. J Pharmacol Exp Ther 303:1029–1037